

# RSC Advances



This is an *Accepted Manuscript*, which has been through the Royal Society of Chemistry peer review process and has been accepted for publication.

*Accepted Manuscripts* are published online shortly after acceptance, before technical editing, formatting and proof reading. Using this free service, authors can make their results available to the community, in citable form, before we publish the edited article. This *Accepted Manuscript* will be replaced by the edited, formatted and paginated article as soon as this is available.

You can find more information about *Accepted Manuscripts* in the [Information for Authors](#).

Please note that technical editing may introduce minor changes to the text and/or graphics, which may alter content. The journal's standard [Terms & Conditions](#) and the [Ethical guidelines](#) still apply. In no event shall the Royal Society of Chemistry be held responsible for any errors or omissions in this *Accepted Manuscript* or any consequences arising from the use of any information it contains.



## RSC ADVANCES

## ARTICLE

## Preparation and pyrolysis characteristics of PNIPAM grafted SiO<sub>2</sub> hollow spheres loading vitamin C

Jing Hu<sup>\*a,b</sup>, Meixia Chen<sup>a</sup>, Huaixiang Tian<sup>a</sup>, Weijun Deng<sup>a</sup>

Received 00th January 20xx,  
Accepted 00th January 20xx

DOI: 10.1039/x0xx00000x

www.rsc.org/

Thermal-responsive poly(N-isopropyl acrylamide) grafted SiO<sub>2</sub> hollow spheres (PSHS) were successfully prepared by multi-step reaction, and then PSHS was used to load vitamin C (VC). Pyrolysis characteristics, kinetic and thermodynamic parameters of PSHS loading VC were measured via thermogravimetric analysis (TGA). Two peaks of 193.03 °C and 247.56 °C were obtained from DTG curve of PSHS loading VC, which were corresponding to the decomposition of the physically absorbed VC and bound VC molecules formed by the hydrogen bond between VC and PSHS dividedly. The average value of activation energy calculated by Coats-Redfern method was 78.91 kJ/mol, equal to the activation enthalpy (77.31 kJ/mol). The activation entropy was -82.60 J/mol-K and the activation free energy was 115.82 kJ/mol. These results proved that VC was encapsulated into PSHS via hydrogen bond and Van der Waals force. Finally, PSHS loading VC exhibited the excellent temperature controllable release property.

### Introduction

As an essential nutrient of human body, VC has diverse functions including an essential role in hydroxylation reactions necessary for collagen formation and carnitine synthesis as well as the facilitation of iron absorption. In particular, VC has the whitening and pale spot effects due to their inoxidizability,<sup>1-3</sup> anti-free radicals ability and inhibiting tyrosinase. However, VC is very unstable to air, light, moisture, heat, oxygen, metal ions and base, and easily decomposed into biologically inactive compounds. To make up for the above disadvantages, liposomes, starches, other biopolymers and inorganic materials have been used to encapsulate VC.<sup>4-11</sup> For instance, Stevanović *et al.*<sup>12</sup> prepared poly(DL-lactide-co-glycolide) nanospheres (110-170 nm) and encapsulated VC in the polymer matrix. These nanospheres encapsulated with VC in the physiological solution (0.9% sodium chloride solution) had been degraded within 8 weeks and fully released all the encapsulated VC. Comunian *et al.*<sup>13</sup> reported that solid lipid microcapsules loading VC with the encapsulation efficiency (96.6%) were fabricated via microfluidic technology. After 30 days, the microcapsules still retained 55.89% VC at 4 °C and 46.06% VC at 20 °C. Palma-Rodriguez and coworkers<sup>14</sup> obtained the microcapsules of VC using rice native starch and acid-treated starches from rice, potato, and maize as wall

materials via spray-drying. These starch microcapsules showed the excellent sustained-release property of VC over the storage of 4 weeks. Shen *et al.*<sup>15</sup> synthesized 395 nm hollow silica spheres with the shell thickness of 9 nm, specific surface areas of 508.9 m<sup>2</sup>/g and average pore diameters of 8.67 nm. Then VC was encapsulated into the mesoporous silica hollow spheres. The release behavior of VC from the spheres fit first-order release model. During the release process, VC moved from the core through the mesopores of shell layer into the solution. The above-mentioned materials released VC depending on the pores of the shell surface or the broken polymer wall at the special condition. Until now, few researches about the encapsulation and release of VC based on the environmental responsive materials have been reported.<sup>16-18</sup> The most common responsive stimulus is temperature. Recently, the thermal-responsive materials loaded with perfumes,<sup>16</sup> fuels<sup>17</sup> and functional enzymes<sup>18</sup> was studied. Our previous study<sup>16</sup> reported that thermal-responsive poly(n-isopropyl acrylamide-co-styrene) hybrid hollow spheres were successfully synthesized via a one-step method and could be used as controllable releasing systems for fragrance compounds, essential oils and so on. However, there is no researches about thermal-responsive materials loading VC. Moreover, it should be note that the kinetic and thermodynamics analysis of thermal-responsive materials loading VC via TGA have not been reported. Poly(N-isopropylacrylamide) (PNIPAM) is the most widely used temperature responsive polymer.<sup>19</sup> PNIPAM exhibits a sharp phase transition with the low critical solution temperature (LCST) at around 32 °C in water.<sup>20</sup> Below the LCST, PNIPAM exists as a flexible conformation and is soluble in water. Above the LCST, the polymer becomes hydrophobic

<sup>a</sup>School of Perfume and Aroma Technology, Shanghai Institute of Technology, Shanghai, 201418, China. <sup>b</sup>Shanghai Research Institute of Fragrance & Flavor Industry, Shanghai, 200232, P. R. China

† Correspondence to: J. Hu (hujing@sit.edu.cn)

Electronic Supplementary Information (ESI) available: [details of any supplementary information available should be included here]. See DOI: 10.1039/x0xx00000x

and the chains collapse. In the present work, thermal-responsive poly(*N*-isopropyl acrylamide) grafted SiO<sub>2</sub> hollow spheres (PSHS) was successfully prepared via multi-step reaction and characterized by transmission electron microscopy (TEM), Fourier transform infrared (FTIR) spectroscopy and thermogravimetric analysis (TGA). Then PSHS was used to load and then release VC using temperature as the trigger. When the temperature was lower than LCST, VC could release from the hollow cavity of the PNIPAM grafted SiO<sub>2</sub> hollow spheres and keep stable. This is attributed to that the molecular chains of PNIPAM would swell below LCST so that the nano-pores of the hollow spheres were open. However, at the temperature above LCST, VC can't release due to the shrinkage of PNIPAM. TGA is a method of thermal analysis in which changes in physical and chemical properties of materials are measured as a function of increasing temperature, or as a function of time. Here, TGA was also used to determinate the kinetic and thermodynamic parameters of PSHS loading VC at the different heating rates. The kinetics parameters were obtained by Coats-Redfern method,<sup>21</sup> Kissinger-Akahira-Sunose (KAS) method<sup>22</sup> and Flynn-Wall-Ozawa (FWO) method.<sup>23</sup> The activation energy, pre-exponential factor, enthalpy, entropy and free energy of activation were obtained by TGA,<sup>24,25</sup> which can be employed to estimate the interaction between PSHS and VC.

## Results and discussion

### Structure and micromorphology of PSHS

Fig. 1(A) and (B), typical TEM images, show the micromorphology of SiO<sub>2</sub> hollow spheres and PSHS. The contrast between the dark shell and the grey core indicates that these spheres are hollow structure. SiO<sub>2</sub> hollow spheres and PSHS are homogeneous. SiO<sub>2</sub> hollow spheres have the average sizes of 186 nm with a shell thickness of 8 nm. After PNIPAM grafted, the average diameter and shell thickness of PSHS increase to 196 nm and 15 nm. Furthermore, it should be noted that there are some "white plots" on the surface of SiO<sub>2</sub> hollow spheres, while the surface of PSHS is more dark and compact. This result can demonstrate that PNIPAM had been grafted SiO<sub>2</sub> hollow spheres successfully.

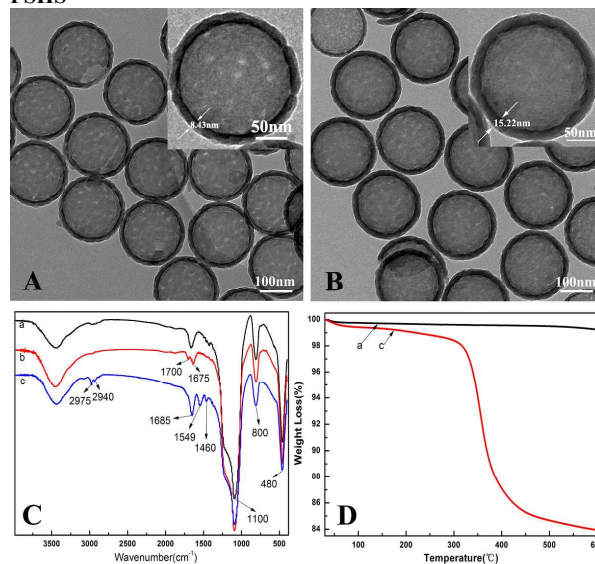
Fig. 1(C) illustrates that the difference among the FTIR spectra of SiO<sub>2</sub> hollow spheres, MPS modified SiO<sub>2</sub> hollow spheres and PSHS. The main absorption bands of silica hollow spheres, Si-O-Si, Si-O bending and Si-O-Si stretching are revealed at 480 cm<sup>-1</sup>, 800 cm<sup>-1</sup> and 1100 cm<sup>-1</sup>, respectively. Besides, the obvious absorption peak at 1690 cm<sup>-1</sup> is shown a solvent hydroxyl stretching. For MPS modified silica hollow spheres, except for the characteristic peaks of SiO<sub>2</sub> hollow sphere, other bands at 1700 cm<sup>-1</sup> and 1675 cm<sup>-1</sup> for the stretching vibration absorptions of C=O and -CH=CH- groups. Compared with SiO<sub>2</sub> hollow spheres and MPS modified SiO<sub>2</sub> hollow spheres, the absorption peak of C=O stretching vibration blueshifts to 1685 cm<sup>-1</sup>, and the

absorption peak at 1549 cm<sup>-1</sup> is assigned to the amide II band, which is a combination of the N-H bending and C-N stretching vibration of PNIPAM chain. The absorption peak at 1460 cm<sup>-1</sup> is attributed to CH<sub>3</sub> bending vibration. In addition, the peaks at 2975 and 2940 cm<sup>-1</sup> corresponds to the asymmetrical and symmetrical stretching vibrations of the CH<sub>2</sub> groups, respectively. From these absorption bands, the surface of SiO<sub>2</sub> hollow spheres has been successfully grafted with PNIPAM.

TGA results of SiO<sub>2</sub> hollow spheres and PSHS are displayed in Fig. 1(D). SiO<sub>2</sub> hollow spheres have no decomposition during the heating process of the samples. However, PSHS has two loss stages. The first stage from room temperature to 320 °C is a slight weight loss (1.67%) for the volatilization of water on the surface and intervals of PSHS. The second stage (320 - 600 °C) is characterized by a major weight loss (14.68%), which belongs to the pyrolysis of PNIPAM. This demonstrates that PNIPAM is grafted onto the surface of SiO<sub>2</sub> hollow spheres successfully.

### Thermogravimetric experiments

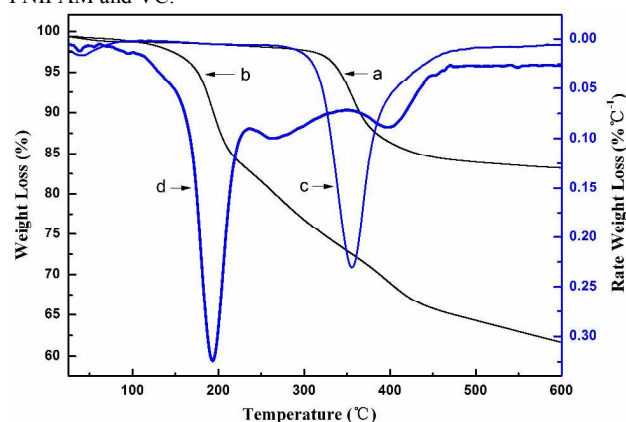
#### Pyrolysis characteristic comparison of PSHS loading VC and PSHS



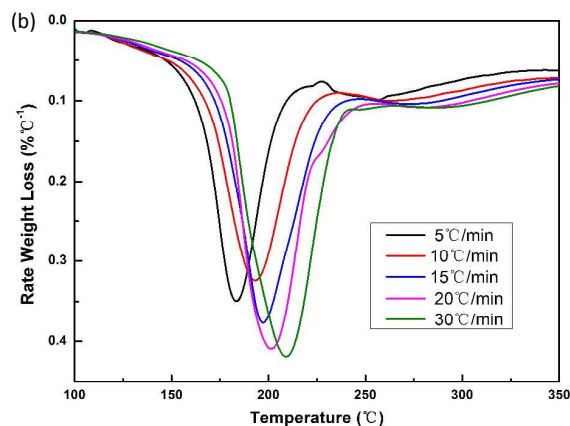
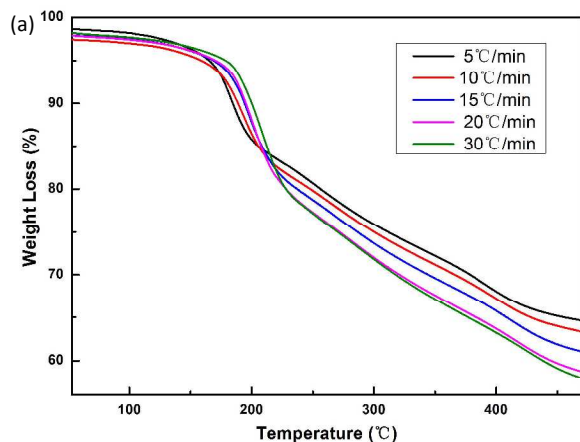
**Fig. 1** Typical TEM images of SiO<sub>2</sub> hollow spheres (A) and PSHS (B), Insets are the corresponding magnified images with a scale bar of 50 nm. FTIR spectra (C) of SiO<sub>2</sub> hollow spheres (a), MPS modified SiO<sub>2</sub> hollow spheres (b) and PSHS (c). TGA curves (D) of SiO<sub>2</sub> hollow spheres (a) and PSHS (c).

Fig. 2 displays the weight loss and the rate of weight loss curves of PSHS and PSHS loading VC under inert atmosphere at a heating rate of 10 °C/min. Compared to the pyrolysis characteristic of PSHS, three main stages can be distinguished from the TG curve of PSHS loading VC. The first stage goes from room temperature to 68.08 °C with a slight weight loss due to the desorption of water. The new second weight loss of PSHS loading VC from 68.08 °C to 320 °C is 23.93 %. This is attributed to the decomposition of VC encapsulated in PSHS.

Furthermore, two peaks can be observed in DTG curve of PSHS loading VC from 68.08 °C to 320 °C. The first strong peak temperature is 193.03 °C and at this temperature the rate of weight loss achieves maximum value (0.32 %/°C). This should be ascribed to the degradation of free VC molecules physically absorbed in the hollow cavity of the silica spheres. The other shoulder peak is at 247.56 °C and the maximum decomposition rate of VC is only 0.11 %/°C. This reflects the thermal degradation of bound VC molecules formed by the hydrogen bonding between PSHS and VC. The third weight loss of PSHS loading VC (10.17 %), ranging from 320 to 600 °C, could be ascribed to the decomposition of PNIPAM grafted on the SiO<sub>2</sub> hollow spheres. During this period, the peak temperature shift to 398.98 °C and the maximum rate of weight loss decreased to 0.09 %/°C from DTG curve of PSHS loading VC. It is concluded that there are some interaction between PNIPAM and VC.



**Fig.2** TG(a and b)-DTG(c and d) curves of PSHS (a and c) and PSHS loading VC (b and d).



**Fig.3** TG curves(a) and DTG curves(b) of PSHS loading VC at different heating rates

#### Effect of heating rate

Fig. 3 shows the weight loss and the rate of weight loss curves obtained from the decomposition of PSHS loading VC at different heating rates (5, 10, 15, 20 and 30 °C/min). The whole curves include a strong peak corresponding to the decomposition of VC. It can be found that the peak shift towards higher temperature when the heating rate is increased. This is typical phenomena for all non-isothermal experiments. The major reason for these phenomena is that PSHS loading VC is a poor conductor of heating. For the PSHS loading VC, there is a temperature gradient throughout the cross-section of the spheres. At lower heating rate, the temperature outline down the cross-section can be hypothesized linear change as both the inner core and the outer surface of the PSHS loading VC reaches to same temperature at a specific time as adequate time is offered to heat, while there exists critical difference in temperature profile along the cross-section of the PSHS loading VC.<sup>26</sup>

#### Kinetic parameters of PSHS loading VC

In consideration of the fact that PSHS loading VC is a mixture composed of easily oxidized VC and PNIPAM, the decomposition of PSHS loading VC comprises a large number of reactions in parallel and in series, whereas DTG measures the overall weight loss rate. DTG, as a result, provides general information on the whole kinetic rather than individual reactions.

TGA is used to measure the kinetic parameters of PSHS loading VC such as activation energy and Arrhenius frequency. The Coats-Redfern method, Kissinger-Akahira-Sunose (KAS) method, and the Flynn-Wall-Ozawa (FWO) method are used to determine the pyrolysis kinetic parameters.

The rate representation for the degradation or conversion,  $da/dt$ , is a linear function of a temperature-dependent rate constant,  $k$  and a function of conversion,  $f(a)$ . The rate of conversion may be expressed by,

$$\frac{d\alpha}{dt} = kf(\alpha) \quad (1)$$

$$f(\alpha) = (1-\alpha)^n \quad (2)$$

where  $\alpha$  is the converted rate of reaction, which is defined as  $(\omega_0 - \omega)/(\omega_0 - \omega_\infty)$ ,  $n$  is the order of reaction,  $\omega_0$  is the mass of initial sample,  $\omega$  is the mass of actual sample at time  $t$ ,  $\omega_\infty$  is the mass of residue at the end of the reaction, and  $k$  is the rate constant, which is also defined by the Arrhenius equation:

$$k = A \exp\left(-\frac{E}{RT}\right) \quad (3)$$

where  $A$  is the pre-exponential factor,  $E$  is the activation energy,  $R$  is the gas constant, and  $T$  is the absolute temperature.

For a linear heating rate of, say,  $\beta \text{ K} \cdot \text{min}^{-1}$ :

$$\beta = \frac{dT}{dt} \quad (4)$$

By combining Eqs. (1) - (4), the reaction rate can be written in the form:

$$\frac{d\alpha}{f(\alpha)} = \frac{A}{\beta} \exp\left(-\frac{E}{RT}\right) dT \quad (5)$$

The integrated form of Eq. (5) is generally expressed as

$$G(\alpha) = \int_0^\alpha \frac{d\alpha}{f(\alpha)} = \frac{A}{\beta} \int_{T_0}^T \exp\left(-\frac{E}{RT}\right) dT = \frac{AE}{\beta R} P\left(\frac{E}{RT}\right) \quad (6)$$

where  $G(\alpha)$  is the integrated form of the conversion dependence function  $f(\alpha)$ . Essentially the technique assumes that the  $A$ ,  $f(\alpha)$  and  $E$  are independent of  $T$ , while  $A$  and  $E$  are independent of  $\alpha$ , then Eq. (6) may be integrated to give the following equation in logarithmic form:

$$\ln G(\alpha) = \ln\left(\frac{AE}{R}\right) - \ln \beta + \ln P\left(\frac{E}{RT}\right) \quad (7)$$

Based on these equations, different kinetic methods have been applied in this study.

#### Coats-Redfern method

Coats-Redfern method is an integral method, and it involves the thermal degradation mechanism. Using an asymptotic approximation for the resolution of Eq. (7) ( $2RT \ll 1$ ), the following equations can be concluded:

$$\ln\left[\frac{1-(1-\alpha)^{1-n}}{T^2(1-n)}\right] = \ln\left(\frac{AR}{\beta E}\right) - \frac{E}{RT} \quad (\text{for } n \neq 1) \quad (8)$$

$$\ln\left[\frac{-\ln(1-\alpha)}{T^2}\right] = \ln\left(\frac{AR}{\beta E}\right) - \frac{E}{RT} \quad (\text{for } n=1) \quad (9)$$

where  $n$  is the order of reaction.

Thus a plot of either  $\ln[(1-(1-\alpha)^{1-n})/T^2(1-n)]$  against  $1/T$  or, where  $n=1$ ,  $\ln[-\ln(1-\alpha)/T^2]$  against  $1/T$  should result in a straight line of slope  $-E/R$  for correct value of  $n$ . In general, it is assumed that devolatilization in the kinetic analysis of DTG data is a first-order reaction. Therefore, the pyrolysis of PSHS loading VC has been regarded as a first-order reaction. If  $2RT \ll 1$ , the activation energy and pre-exponential factor can be obtained from the slope and intercept of the line, respectively. Plots of  $\ln[-\ln(1-\alpha)/T^2]$

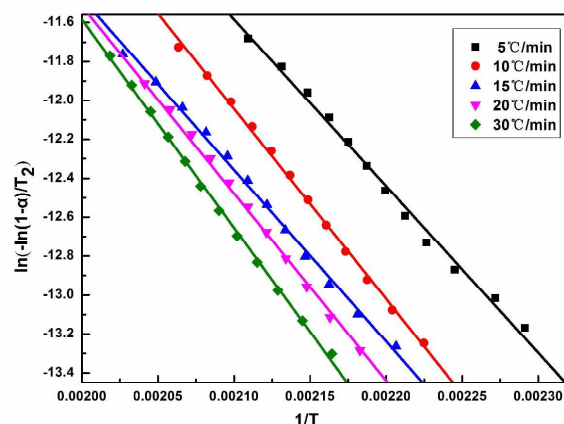


Fig. 4 Plots of  $\ln[-\ln(1-\alpha)/T^2]$  vs.  $1/T$  at different heating rates by Coats-Redfern method

against  $1/T$  is shown in Fig. 4. There is a good linear relationship between  $\ln[-\ln(1-\alpha)/T^2]$  and  $1/T$  at different heating rates from  $5^\circ\text{C}/\text{min}$  to  $30^\circ\text{C}/\text{min}$ . The values of activation energy and pre-exponential factor calculated by Coats-Redfern method are shown in Table 2. The whole plots have a high linear correlation coefficients greater than 0.99, so the assumption on a first-order reaction is feasible. The apparent activation energies of PSHS loading VC are 71.18–88.87 kJ/mol. Meanwhile, the apparent activation energy mainly tends to increase with the heating rates increased. Generally, the smaller the activation energy is, the more easily the reaction performs. Small activation energy demonstrates that VC can be decomposed from PSHS easily. While the high activation energy indicates that VC is encapsulated in PSHS firmly. This can provide an ideal model for the temperature-controllable release of PSHS loading VC.

#### Kissinger-Akahira-Sunose (KAS) and Flynn-Wall-Ozawa (FWO) methods

The KAS method is based on the Coats-Redfern approximation.<sup>16</sup> It follows that:

$$P\left(\frac{E}{RT}\right) \approx \frac{\exp(-E/RT)}{(E/RT)^2} \quad (10)$$

From relationships (7) and (10), it follows that:

$$\ln \frac{\beta}{T^2} = \ln \frac{AR}{EG(\alpha)} - \frac{E}{RT} \quad (11)$$

Therefore, the plots  $\ln(\beta/T^2)$  versus  $1/T$  for a constant value of  $\alpha$  should be a straight line whose slope can be used to evaluate the activation energy.

The FWO method is derived from integral isoconversional method. Using Doyle's approximation for the integral which allows  $(\ln P(E/RT) \approx -5.331 - 1.052(E/RT))$ ,<sup>27</sup> Eq. (7) can be simplified as

$$\ln \beta = \ln \frac{AE}{RG(\alpha)} - 5.331 - 1.052 \frac{E}{RT} \quad (12)$$

Therefore, for  $\alpha = \text{constant}$ , the plots  $\ln \beta$  versus  $1/T$ , obtained from thermograms recorded at five heating rates,

should be a straight line whose slope can be used to estimate the activation energy. Therefore, the activation energy can be obtained via KAS method and FWO method without the previous knowledge of the reaction mechanism, which is different from the Coats-Redfern method.

In accordance with Eqs. (10) and (11), plots of  $\ln(\beta/T^2)$  against  $1/T$  or  $\ln\beta$  against  $1/T$  are shown in Fig. 5, which displays the representative plots for the main stage of VC weight loss. The activation energy of PSHS loading VC degradation at different conversion  $\alpha$  can be obtained from the slope of line in Fig. 5.

Table 3 shows the activation energies of the PSHS loading VC are 105.17-125.78 kJ/mol (by KAS method) and 108.53-128.17 kJ/mol (by FWO method) at various conversions. Most of the plots have fairly high linear correlation coefficients greater than 0.99, and the average values of activation energy between the

KAS and FWO methods has no significantly difference. The activation energies slightly varied with the degree of conversion, indicating that there exists a high probability for the presence of a single-step reaction.<sup>28</sup> When compared the kinetic activation energy values obtained by KAS and FWO methods with those calculated by Coats-Redfern method, it can be found that the activation energy values by the KAS and FWO method are larger than those by the Coats-Redfern method (71.18 kJ/mol to 88.87 kJ/mol). This phenomenon is in accordance with the results of the previous literatures and may be caused by the applies of different kinetic methods.<sup>29,30</sup> Meanwhile, all the plots calculated by the Coats-Redfern method have high linear correlation coefficients greater than 0.99, which demonstrated that Coats-Redfern method is suitable to investigate the pyrolysis kinetics of PSHS loading VC.

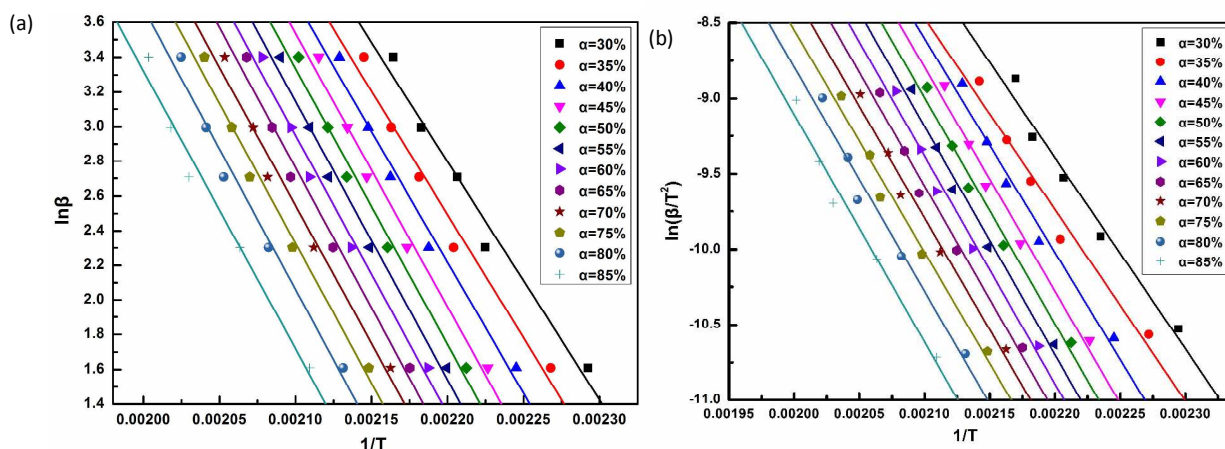


Fig. 5 (a) Plots of  $\ln\beta$  vs.  $1/T$  at different  $\alpha$  by FWO method and (b) plots of  $\ln(\beta/T^2)$  vs.  $1/T$  at different  $\alpha$  by KAS method

Table 2 The pyrolysis kinetic parameters of PSHS loading VC calculated by Coats-Redfern method

Heating rate $\beta$	Temperature range (°C)	$\alpha$ (%)	$E$ (kJ/mol)	$A$ ( $s^{-1}$ )	$R$
5	158.96-200.95	30-85	71.18	$2.56 \times 10^7$	-0.9967
10	176.32-211.48	30-85	81.25	$4.71 \times 10^8$	-0.9991
15	180.06-220.22	30-85	73.28	$6.21 \times 10^7$	-0.9981
20	184.97-222.39	30-85	79.96	$4.33 \times 10^8$	-0.9976
30	188.89-222.27	30-85	88.87	$5.75 \times 10^9$	-0.9993
Average		30-85	78.91	$1.35 \times 10^9$	

### Thermodynamic parameters of PSHS loading VC

Enthalpy of activation is a measure of the total energy of a thermodynamic system. The relationship among enthalpy of activation, activation energy and temperature can be expressed as Eq. (13).

$$\Delta H^\ddagger = E - RT \quad (13)$$

$\Delta H^\ddagger$  can be obtained by solving Eq. (13)

Entropy of activation is a measure of the number of specific ways in which a system may be arranged, often taken to be a measure of disorder, confusion, and disorganization. The

relationship among entropy of activation, pre-exponential factor and temperature can be expressed as Eq. (14).<sup>31</sup>

$$A = \frac{k_B T}{h} \exp\left(\frac{\Delta S^\ddagger}{R}\right) \quad (14)$$

Where  $h$  is Plank constant,  $k_B$  is Boltzmann constant.

Changing Eq. (14) gives Eq. (15)

$$\Delta S^\ddagger = R \ln\left(\frac{Ah}{k_B T}\right) \quad (15)$$

$\Delta S^\ddagger$  can be obtained by solving Eq. (15)

Free energy is a thermodynamic potential that measures the “usefulness” or process-initiating work obtainable from a thermodynamic system at a constant temperature and pressure. The relationship among free energy of activation, enthalpy of activation and entropy of activation can be expressed as Eq. (16)

$$\Delta G^\ddagger = \Delta H^\ddagger - T\Delta S^\ddagger \quad (16)$$

$\Delta G^\ddagger$  can be obtained by solving Eq. (16). According to Eq. (13) - (16), the enthalpy of activation ( $\Delta H^\ddagger$ ) is 77.31 kJ/mol, which is approximately equal to the energy activation calculated by Coats-Redfern method. Moreover, the value of  $\Delta S^\ddagger$  (-82.60 J/mol·K) decreases in the pyrolysis process of the PSHS loading VC. This indicates that VC has been gradually decomposed. The free energy of activation ( $\Delta G^\ddagger$ ) is 115.82 kJ/mol, which illustrates that the pyrolysis process of PSHS loading VC is a non-spontaneous process. VC has been encapsulated in PSHS firmly and it can't release from PSHS loading VC at the temperature above LCST.

#### Thermal-response and controllable release of PSHS loading VC

PNIPAM is a temperature-responsive polymer, which exhibits a sharp phase transition from a hydrophilic, water-swollen state to a hydrophobic, globular state when heated to above its lower critical solution temperature (LCST), about 32 °C in water. As

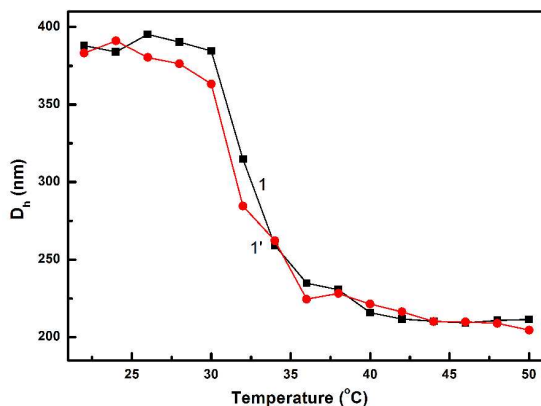


**Fig.6** The hydrodynamic diameter of PSHS as a function of temperature. (1) from 22 to 50 °C, (1') from 50 to 22 °C

shown in Fig.6(1), the mean diameter of PSHS changes sharply at 30 °C in water. When the temperature is lower than 30 °C, PNIPAM chains grafted on SiO<sub>2</sub> hollow spheres are swollen to make the nanopores on the hollow spheres open and increase the average size of PSHS. At temperature above 30 °C, PNIPAM chains collapse to cover the nano holes. When PSHS is cooled to the original 22 °C, the mean size of spheres is reverted to their original one, indicating a reversible swelling and shrinking process (Fig.6, 1').

The controllable release properties of PSHS loading VC at 20 °C and 50 °C have been determined as shown in Fig. 7. In the first 2h, the release rates of VC from PSHS at 20 °C and 50 °C are similar due to the release of some VC molecules encapsulated in PNIPAM layer. Then, PSHS loading VC at 20 °C releases sharply in the following time, and finally liberates 71.72% after 24h. This is attributed to that PNIPAM chains are swollen with opening the nanopores on PSHS. However, when the temperature is improved to 50 °C, the release of VC in PSHS slows down and then reaches the equilibrium (38.95% after 24h). The decrease of VC release rate at the high temperature should be attributed to that the PNIPAM chains collapse so that the tunnels on the shell of the hollow spheres are close.

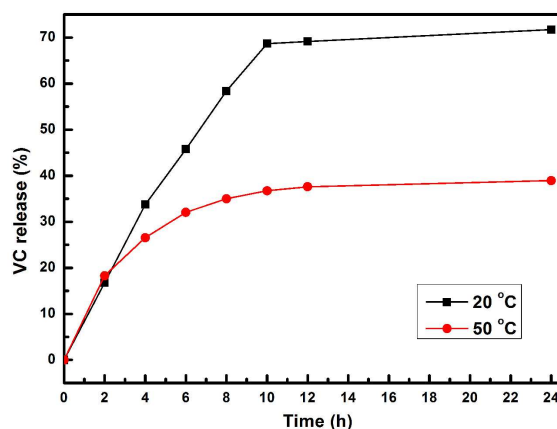


**Fig.7** VC release of PSHS loading VC at 20 °C and 50 °C

**Table 3** The pyrolysis kinetic parameters of PSHS loading VC calculated by KAS and FWO method

Conversion rate (%)	KAS method		FWO method	
	E (kJ/mol)	R	E (kJ/mol)	R
30	105.17	-0.9878	108.53	-0.9882
35	105.42	-0.9869	112.50	-0.9885
40	117.83	-0.9899	119.23	-0.9911
45	123.42	-0.9912	124.57	-0.9921
50	124.62	-0.9920	125.78	-0.9929
55	125.78	-0.9925	126.93	-0.9932
60	125.56	-0.9922	126.76	-0.9930

65	125.00	-0.9910	127.80	-0.9911
70	123.06	-0.9915	125.92	-0.9904
75	122.44	-0.9901	127.44	-0.9921
80	123.60	-0.9871	128.17	-0.9910
85	125.29	-0.9895	126.74	-0.9896
Average	120.60		123.36	

## Experimental

### Materials

Styrene (ST,  $\cong$  99.0%), tetraethoxysilane (TEOS,  $\cong$  28.4%), aqueous ammonia solution (28 wt%) and absolute ethanol ( $\cong$  99.7%) were purchased from Shanghai Chemical Reagent Co. Ltd. (China). Methacryloxyethyl ammonium chloride (MTC, 80%), 3-(trimethoxysilyl)propyl methacrylate (MPS, 97.0%), N-isopropyl acrylamide (NIPAM, 98.0%),  $\alpha,\alpha'$ -azodiisobutyramidine dihydrochloride (AIBA,  $\cong$  98.0%), 2,2'-Azobis(2-methylpropionitrile) (AIBN,  $\cong$  99.8%) and poly(vinyl pyrrolidone) with a molecular weight of 30000 (PVP, K30) and ascorbic acid (AA,  $\cong$  98.0%) were supplied by Sigma-Aldrich Co. Ltd.. Deionized water was used throughout the experiment. All of the reagents were used without further purification.

### Synthesis of polystyrene (PS)

In a typical experiment, 10 g ST, 0.1 g MTC (cationic monomer), 1.5 g PVP (dispersing agent) and 90 g H<sub>2</sub>O were added sequentially into a 250 mL three-neck flask equipped with a mechanical stirrer, an N<sub>2</sub> inlet, a thermometer with a temperature controller, a Graham condenser, and a heating mantle. The mixture solution was purged with bubbling nitrogen gas under a stirring rate of 300 rpm for 30 min at room temperature. After heating the solution to 70 °C, the initiator of 0.26 g AIBA aqueous solution (2.6 wt%) was added to the system. The mixture reacted at 70 °C under stirring for 8 h. The reaction product was centrifuged at 14500 rpm for 45 min, then redispersed in absolute ethanol and subjected to three more cycles of centrifugation/wash before further use.

### Synthesis of SiO<sub>2</sub> hollow spheres

Typically, 4.2 wt% PS absolute ethanol solution was stirred mechanically at a rate of 250 rpm equipped with a Graham condenser. This system was heated up to 50 °C, followed by the addition of 12.7 wt% TEOS absolute ethanol solution and 39.1 % aqueous ammonia solution, and stirred at that temperature for 48 h to obtain PS@SiO<sub>2</sub> hybrid particles. These spheres were treated with three more cycles of centrifugation/wash, then dried entirely in the oven at 80 °C and calcined at 550 °C for 8 h to obtain SiO<sub>2</sub> hollow spheres.

### Synthesis of PSHS

10 g SiO<sub>2</sub> (1wt%) hollow spheres absolute ethanol solution, 0.8 g MPS and 1.0 g H<sub>2</sub>O was added into a 100 mL round-bottom flask with magnetic stirring. Then the system was heated up to 60 °C and reacted at that temperature for 24 h. MPS modified SiO<sub>2</sub> hollow spheres were prepared. PSHS were synthesized by radical copolymerization of MPS modified hollow silica with

NIPAM monomers. First, 10 g MPS modified SiO<sub>2</sub> (1 wt%) absolute ethanol was added into a 100 mL three-neck flask equipped with a mechanical stirrer, an N<sub>2</sub> inlet, a thermometer with a temperature controller, a Graham condenser, and a heating mantle. After, the reagent mixture was purged with nitrogen under a stirring rate of 250 rpm for 1h at room temperature. Next, the system was heated up to 65 °C and continue stirred for 0.5 h. Then, the monomer of NIPAM ethanol solution (3 g, 16.7 wt%) and initiator of AIBN ethanol solution (2 g, 1.2 wt%) were injected simultaneously into the reaction vessel within 0.5 h. Finally, the polymerization was carried out at 70 °C for 8 h. PSHS were centrifuged at 12000 rpm for 15 min and washed several times with water to remove the remainders.

### PSHS loading VC and its controllable release

Typically, 10 g/L VC aqueous solution was prepared. Then, 0.02 g thermo-responsive PSHS and 25 mL VC aqueous solution were added into a 50 mL conical flask, and stirred at 400 rpm for 24 h at room temperature. The obtained PSHS loading VC were centrifuged at 12000 rpm for 15 min and washed several times with water to remove unreacted residues. The thermal-responsive release of VC in PSHS was determined by UV-Vis-NIR absorption spectroscopy with a Hitachi U-4100 spectrophotometer. PSHS loading VC was redispersed into water. A vial containing the above solution was kept at the desired temperature; the aliquots of supernatant were taken at time intervals. Meanwhile, fresh water was supplemented into each sample was taken to keep the total volume of the suspension constant. The released quantity of VC was estimated based on the absorbance of the separated supernatant solution. Cumulative release was expressed as the released total percentage of VC.

### Characterization

The chemical structures of the as-obtained products were analyzed by FTIR spectroscopy (VETOR-7, Bruker, Germany). The micromorphology and structure of the as-obtained spheres were observed via an H-600 electron microscope (Hitachi, Japan). A TGA-Q5000IR thermogravimetric analyzer (TA Instruments, USA) was used to investigate the kinetic pyrolysis characteristics. In each experiment, about 5 mg of samples were spread uniformly on the bottom of the ceramic crucible of the thermal analyzer. The pyrolysis experiments were performed at heating rates of 5, 10, 15, 20 and 30 °C/min in a dynamic high purity nitrogen flow of 20 ml/min. The temperature of the

furnace was programmed to rise from room temperature to 600 °C.

## Conclusions

Thermal-responsive PNIPAM grafted SiO<sub>2</sub> hollow spheres (PSHS) were successfully prepared by multi-step reaction, and applied to load VC in an aqueous solution directly. TEM indicated that the shell thickness of PSHS increased by 6.79 nm after the copolymerization of PNIPAM. FTIR spectroscopy illustrated that PNIPAM was grafted onto the surface of SiO<sub>2</sub>. TGA was used to determinate kinetic and thermodynamic parameters of PSHS loading VC at different heating rates. Coats-Redfern method was suitable to investigate the pyrolysis kinetics of PSHS loading VC. The apparent activation energy mainly tends to increase with the heating rates increased. The average values of activation energy by Coats-Redfern method were 78.91 kJ/mol, which was equal to the enthalpy of

activation (77.31 kJ/mol). The entropy of activation was -82.60 J/mol-K and the free energy of activation was 115.82 kJ/mol. This proved that VC was encapsulated into PSHS firmly and the interaction between VC and PSHS could be ascribed to the non-covalent interactions including hydrogen bond and Van der Waals force. Finally, PSHS loading VC at 20 °C released 71.72% after 24h, but during this period PSHS loading VC only liberated 38.95% at 50 °C. The study of pyrolysis characteristics, kinetics and thermodynamic parameters provides a novel method to study the interaction mechanism between VC and thermal responsive encapsulated materials.

## Acknowledgements

Financial supports from the National Natural Science Foundation of China (21106084, 31401535), Science and Technology Foundation of Shanghai (14zz164, 14ZR1440400) and Shanghai Rising-Star Program (14QA1403300) are appreciated.

## References

- 1 A. Bendich, L. J. Machlin and O. Scandurra, *Free Radical Biol. Med.*, 1986, **2**, 419-444.
- 2 T. Doba, G. W. Burton and K. U. Ingold, *Biochim. Biophys. Acta*, 1985, **835**, 298-303.
- 3 Z. H. Kuanga, P. F. Wang and R. L. Zheng, *Chem. Phys. Lipids*, 1994, **71**, 95-97.
- 4 I. Yamamoto, A. Tai, Y. Fujinami, K. Sasaki and S. Okazaki, *J. Med. Chem.*, 2002, **45**, 462-468.
- 5 M. Gallarate, M. E. Carlotti, M. Trotta and S. Bovo, *Int. J. Pharm.*, 1999, **188**, 233-241.
- 6 R. Austri, A. Semenzato and A. Bettero, *J. Pharm. Biomed. Anal.*, 1997, **15**, 795-801.
- 7 P. Spiclin, M. Gasperlin and V. Kmetec, *Int. J. Pharm.*, 2001, **222**, 271-279.
- 8 E. Jiménez-Fernández, M. Ponce, A. Rodríguez-Rúa, E. Zuasti, M. Manchado and C. Fernández-Díaz, *Aquaculture*, 2015, **443**, 65-76.
- 9 L. F. Hu, M. Chen, W. Z. Shan, T. R. Zhan, M. Y. Liao, X. S. Fang, X. H. Hu and L. M. Wu, *Adv. Mater.*, 2012, **24**, 5872-5877.
- 10 M. Chen, L. F. Hu, J. X. Xu, L. M. Wu and X. S. Fang, *Small*, 2011, **7**, 2449-2453.
- 11 Z. X. Wang, L. M. Wu, M. Chen and S. X. Zhou, *J. Am. Chem. Soc.*, 2009, **131**, 11276-11277.
- 12 M. Stevanović, J. Savić, B. Jordović and D. Uskoković, *Colloid. Surface. B*, 2007, **59**, 215-223.
- 13 T. A. Comunian, A. Abbaspourrad, C. S. Favaro-Trindade and D. A. Weitz, *Food Chem.*, 2014, **152**, 271-275.
- 14 H. M. Palma-Rodriguez, E. Agama-Acevedo, R. A. Gonzalez-Soto, E. J. Vernon-Carter, J. Alvarez-Ramirez and L. A. Bello-Perez, *Starch/Stärke*, 2013, **65**, 584-592.
- 15 B. H. Shen, M. L. Hsieh, H. Y. Chen and J. Y. Wu, *J. Polym. Res.*, 2013, **20**, 1-11.
- 16 J. Hu, L. Q. Liu, Y. Y. Xie and L. M. Wu, *Polym. Chem.*, 2013, **4**, 3293-3299.
- 17 Z. F. Li, K. Geisel, W. Richtering and T. Ngai, *Soft Matter*, 2013, **9**, 9939-9946.
- 18 H. Lomas, I. Canton, S. MacNeil, J. Du, S. P. Armes, A. J. Ryan, A. L. Lewis and G. Battaglia, *Adv. Mater.*, 2007, **19**, 4238-4243.
- 19 E. S. Gil and S. A. Hudson, *Prog. Polym. Chem.*, 2004, **29**, 1173-1222.
- 20 H. G. Schild, *Prog. Polym. Chem.*, 1992, **17**, 163-249.
- 21 A. W. Coats and J. P. Redfern, *Nature*, 1964, **201**, 68-69.
- 22 H. E. Kissinger, *Anal. Chem.*, 1957, **29**, 1702-1706.
- 23 J. H. Flynn and A. L. Wall, *Polym. Lett.*, 1966, **4**, 323-328.
- 24 G. Y. Zhu, X. Zhu, Z. B. Xiao, R. J. Zhou and F. P. Yi, *Waste Manage. (Oxford)*, 2012, **32**, 2287-2293.
- 25 G. Y. Zhu, X. Zhu, Z. B. Xiao and F. P. Yi, *J. Anal. Appl. Pyrol.*, 2012, **94**, 126-130.
- 26 S. Maiti, S. Purakayastha and B. Ghosh, *Fuel*, 2007, **86**, 1513-1518.
- 27 C. Doyle, *J. Appl. Polym. Sci.*, 1961, **5**, 285-292.
- 28 S. Vyazovkin, *Thermochim. Acta*, 2000, **355**, 155-163.
- 29 Y. F. Shih, *Macromol. Chem. Phys.*, 2005, **206**, 383-392.
- 30 Y. F. Shih and R. J. Jeng, *Polym. Degrad. Stabil.*, 2006, **91**, 823-831.
- 31 R. Z. Hu and Q. Z. Shi, (2001). Thermal analysis kinetics. Beijing: Science press (in Chinese).